

Dye adsorption using low cost carbon adsorbent from agrowaste -pearl millet cob husk

Samir Charola, Prasanta Das & Subarna Maiti*

Process Design & Engineering Cell, CSIR-Central Salt & Marine Chemicals Research Institute,
G.B. Marg, Bhavnagar 364002, Gujarat, India

E-mail:smaiti@csmcri.res.in

Received 15 February 2017; accepted 18 October 2018

Activated carbon (MHAC) has been derived from the millet cob husk in a single step activation at a temperature of 600°C, impregnation ratio of 2:1 and residence time of 120 min. The Brunauer–Emmett–Teller (BET) surface area of the MHAC is 1342 m²/g and the scanning electron microscopy (SEM) images and Fourier-transform infrared spectroscopy (FT-IR) are similar to commercial activated carbon. The dye removal performance of the generated carbon has been investigated using methylene blue (MB) using following parameters; contact time, initial concentration of MB, pH and temperature. Langmuir, Freundlich, Temkin and Dubinin–Radushkevich (D-R) adsorption isotherms and three kinetic models have been studied. The adsorption equilibrium data is best fitted to Langmuir isotherm with R² value of 0.972. The adsorption kinetics show that pseudo-second-order kinetic model fits better with the experimental data of MB adsorption by MHAC than pseudo-first-order kinetic model. Regeneration of the carbon has been carried out for five cycles and 85.34 % MB could be adsorbed by the spent carbon; after fifth cycle.

Keywords: Single step activation, Adsorption isotherms, Adsorption kinetics, Millet cob husk, Regeneration

With the expansion of textile and allied industries, the associated waste water pollution problem has faced serious attention. Generally, a dye molecule is a very complex organic substance and therefore not degraded easily¹. Because of its structural stability it creates harmful effects on the environment and human health². There are many methods generally used to remove dye from the wastewater e.g. froth flotation³, membrane separation^{4,5}, air flotation⁶, photo degradation⁷, extraction⁸, biological⁹, chemical oxidation⁹ etc. Out of the above processes, adsorption can be considered as a simple and practical option¹⁰. The usage of activated carbon as an adsorbent is high due to its good thermal stability, high surface area and rich porous structure. Commonly, commercial activated carbon is prepared from the conventional sources like carbonized low grade coal, wood or coconut shell. There is an opportunity for researchers to find out effective and cheap resource to replace the conventional ones¹¹. The ability of adsorption of dye from wastewater mainly depends on the characteristics of the precursor and the preparing conditions¹². Recent studies have focused on the preparation of activated biochar from agricultural residues. Prior work has been done using peanut hull, fruit shell, rice husk, sugarcane leaves, and bamboo as other cheaper sources¹³⁻¹⁶. There are two methods of

activation: Physical activation and chemical activation. Physical activation comprises pyrolysis (below 600°C) and then gasification using oxidizing agents such as steam, CO₂, air or mixture of them at elevated temperature (below 1100°C). In chemical activation, chemicals like KOH, H₃PO₄, ZnCl₂ etc. are commonly used as oxidizing agents¹⁷⁻²². The important benefits of chemical activation are development of rich porous structure in the resulting carbon, high yield and requirement of lower activation temperatures.

In this work, porous activated carbon (MHAC) was derived from millet cob husk using KOH as an oxidizing agent. Production of millet pearl is high in western part of India during to favourable climatic conditions. For separation of pearl millet from the cob, mechanical threshers are used. Millet cob husk and millet pearl are produced after threshing operation. The RPR (residue to product ratio) for cob husk to pearl millet is 1:3^{23,24}. The husk is generally burnt in field and this was selected as precursor of activated carbon. Food chain is not also affected by using millet cob husk as a predecessor for production of MHAC.

Little or no information is reported in literature on the effects of activation conditions: temperature, residence time and impregnation ratio on the physico-chemical properties of carbon produced by activation

of pearl millet cob husk by KOH. The objective of the present study was to determine the optimum value of each process parameter and to investigate the effect of initial dye concentration, contact time and pH on the adsorption of dye. Also, the study of adsorption isotherm, kinetics and thermodynamics was carried out to understand the adsorptive behaviour of the prepared MHAC. The dye chosen for the study was Methylene blue (MB)- a basic dye which has been studied extensively²⁵⁻³². It is most applicable in cotton and synthetic fibers. It has tendency to cause eye burning, vomiting, nausea, diarrhea, profuse sweating, gastritis and mental confusion and hence is an important pollutant.

Experimental Section

Materials

The millet cob husk powder was collected from an agricultural field of Gujarat, a state in western India. In order to remove dirt and other water soluble impurities, it was washed with water and the washed precursor was dried overnight at 105°C in hot air oven. The precursor was then preserved in desiccator to keep away the moisture. Potassium hydroxide (KOH) and hydrochloric acid (HCl) were obtained from Rankem, India. The inert atmosphere during activation was provided by 99.5% pure nitrogen gas. Deionized water was used in this study.

Preparation of activated carbon

The dried millet cob husk was sieved through 100 mesh screen. It was then impregnated with KOH solution for 24 h at room temperature and then dried at 105°C in hot air oven. The impregnated biomass was inserted in a horizontal tube furnace made from stainless steel. The internal diameter and length of tube furnace was 0.03 m and 1 m, respectively. The sample was heated at desired temperature with desired residence time under inert atmosphere. The rate of heating of tube furnace was 10°C/min. After cooling down to room temperature the resultant mixture was thoroughly washed with mild HCl followed by hot distilled water until pH was neutral. The resulting MHAC was again dried at 105°C for 10 h in oven and stored in container for further use. The schematic diagram for the preparation of MHAC is shown in Fig. 1.

Characterization of MHAC

All physico-chemical properties of MHAC were measured precisely. A pH meter, Model Orion STAR A111 (Thermo Fisher Scientific, India) was used to determine the pH of MB solution. BET surface area

and pore size of MHAC was determined by Monosorb Rapid Surface Area Analyzer (Quantachrome Instruments) with the accuracy of 0.01 m²/g. An automatic proximate analyzer, Model APA 2 (Advance Research Instruments Co., India) was used to carry out proximate analysis of MHAC. The minimum detection limit and the temperature accuracy of furnace is 0.2% and ±5°C respectively. The ultimate analysis of MHAC was performed using vario MICRO cube (Elementar, Germany). The surface morphology of porous MHAC was characterized with Field Emission Scanning Electron Microscope, Model JSM-7100F (JEOL, USA). The resolution range from 1.2 nm to 3.0 nm and magnification range in between 10 to 1 million times. The Fourier transform-infrared (FT-IR) spectrum of MHAC was done using a Perkin-Elmer spectroscope (Spectrum GX, Germany) at a resolution of 4 cm⁻¹.

Adsorption study

In this work, the adsorption ability of MHAC was determined by using MB as an adsorbate. The chemical formula of MB is C₁₆H₁₈ClN₃S, a cationic dye having molecular weight of 319.87 g/mol and CI No. 52015.

The 250 mL Erlenmeyer flasks were used to perform all adsorption experiments. Each flask contained 0.15 g of MHAC and 150 mL MB solution of predefined concentrations. The pH of the solution was maintained using 0.1 N NaOH and 0.1 N HCl solutions. Vibrating shaker was employed to shake the flask at the speed of 120 rpm for 24 h. The resultant mixtures after adsorption were then centrifuged at 3500 rpm and the supernatants were studied by UV-Vis spectrophotometer (Orion Aquamate 8000, Thermo Scientific, India) at 665 nm.

The equilibrium adsorption capacity per unit mass of MHAC was computed as follows:

$$q_e = \frac{(C_o - C_e)}{w} \times V \quad \dots (1)$$

where, q_e is the equilibrium adsorption capacity (mg/g), C_o and C_e are the initial and equilibrium concentration of MB (mg/L), respectively, w is the mass of MHAC (g) and V is the volume of sample (mL).

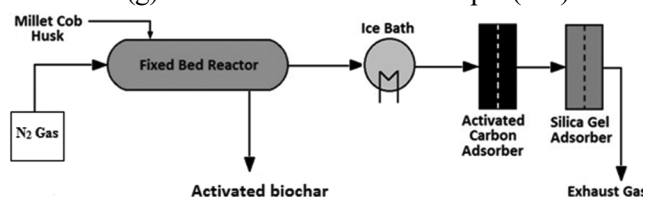


Fig. 1 — Process flow diagram of activation of biomass (Millet cob husk)

The MB removal percentage was estimated as follows:

$$R = \frac{(C_o - C_t)}{C_o} \times 100\% \quad \dots (2)$$

where, C_o and C_t are the initial and t-time concentration of MB (mg/L) respectively and R is the MB removal percentage (%).

Adsorption Isotherm model

The isotherm study is important to investigate the adsorption process. It is also important for optimization of the adsorption system design. In present work, data of equilibrium of MB adsorption were analyzed by four common and widely used adsorption isotherm models: Langmuir, Freundlich, Temkin and Dubinin–Radushkevich (D-R) isotherms. The obtained results were compared with commercial activated carbon (CAC) from Sigma Aldrich of surface area, 750 m²/g.

Langmuir isotherm assumes there is negligible interaction among the adsorbed molecules, all active sites are energetically equal and only one molecule can be handled by each site³³. The linear form of this isotherm equation is expressed as,

$$\frac{1}{q_e} = \frac{1}{Q_o} + \frac{1}{Q_o K_L C_e} \quad \dots (3)$$

where, C_e (mg/L) is the equilibrium concentration of the MB, q_e (mg/g) is the equilibrium adsorption capacity, Q_o (mg/g) and K_L (L/mg) are the monolayer adsorption capacity and Langmuir constants, respectively.

The important characteristics of Langmuir isotherm can be expressed by a unitless parameter called separation factor, R_L , defined as Table 1,

$$R_L = \frac{1}{1 + (K_L C_o)} \quad \dots (4)$$

Freundlich model is based on an empirical equation. It assumes that the adsorption is carrying out on a heterogeneous surface. Each available active site has varying affinities and this binding affinities decrease as the degree of site occupation increases³⁴.

Table 1 — Relation of equilibrium parameter R_L with type of isotherm in Langmuir model

Value of equilibrium parameter	Type of isotherm
$R_L > 1$	Unfavourable
$R_L = 1$	Linear
$0 < R_L < 1$	Favourable
$R_L = 0$	Irreversible

The linear logarithmic form of this isotherm can be expressed as,

$$\ln q_e = \ln K_f + \frac{1}{n} \ln C_e \quad \dots (5)$$

where, K_f is the distribution co-efficient and n is the heterogeneous intensity factor which provides information regarding the adsorption process possibility.

The linear form of Temkin isotherm³⁵ is as follows:

$$q_e = \frac{RT}{b_T} \ln A_T + \frac{RT}{b_T} \ln C_e \quad \dots (6)$$

where, A_T is the binding constant (L/g), b_T is the Temkin isotherm constant, R is the gas constant (8.314 J/mol.K), $B (RT/A_T)$ is the constant related to heat of sorption (J/mol) and T is the temperature (298 K).

Dubinin–Radushkevich isotherm³⁶ can be defined as,

$$\ln q_e = \ln q_s - K_{DR} \varepsilon^2 \quad \dots (7)$$

where ε can be estimated as,

$$\varepsilon = RT \ln \left(1 + \frac{1}{C_e} \right) \quad \dots (8)$$

where, T is the absolute temperature (K) and R is the gas constant (8.314 J/mol.K).

The mean free energy, E can be estimated by:

$$E = \frac{1}{\sqrt{2K_{DR}}} \quad \dots (9)$$

Adsorption kinetics model

The adsorbate uptake rate on adsorbent was described by the kinetics of adsorption. In this study, the rate of adsorption of MB on MHAC was analyzed by three different kinetic models: pseudo-first-order³⁷, pseudo-second-order³⁸ and intraparticle diffusion model³⁹. The linear form of pseudo-first order, pseudo-second-order and intraparticle diffusion model is expressed by equations (10), (11) and (12), respectively.

$$\ln(q_e - q_t) = \ln q_e - k_1 t \quad \dots (10)$$

$$\frac{t}{q_t} = \frac{1}{k_2 q_e^2} + \frac{t}{q_e} \quad \dots (11)$$

$$q_t = k_{int} * t^{0.5} + C_i \quad \dots (12)$$

where, q_e and q_t (mg/g) are the amounts of MB adsorbed at equilibrium and at any time, t (h), respectively, k_1 (h⁻¹), k_2 (g/mg.h) and k_{int} (mg/g.(h)^{1/2}) are the kinetic rate constant for pseudo-first-order, pseudo-second-order and intraparticle diffusion model, respectively and C_i (mg/g) is the intraparticle diffusion model constant.

Results and Discussion

Effect of process parameters on preparation of activated carbon

The pore structure and surface area of activated carbon mainly depends on the activation condition under which it is prepared. The effect of these conditions like temperature, impregnation ratio and residence time on the q_e and also removal percentage of MB, by the carbon was thoroughly studied.

When the impregnation ratio was raised from 1:1 to 2:1, the value of q_e improved from 84.21 mg/g to 249.45 mg/g and the MB removal percentage also upsurged from 50.43 to 99.35%. But, when the impregnation ratio was raised from 2:1 to 3:1, the value of q_e dropped from 249.45 mg/g to 150.01 mg/g and the MB removal percentage also dropped from 99.45 to 66.82%. The above results indicated that the impregnation ratio is one of the crucial parameter for the preparation of activated carbon. Theoretically, it can be inferred that two type of phenomena occurred during the process of chemical activation. In the first step, there was development of mesoporic structure which improved the surface area and the value of q_e . In the second type, enhancement of width of pores occurred which reduced the surface area and value of q_e .

When the activation temperature was increased from 500°C to 600°C at the impregnation ratio of 2:1 and residence time of 120 min, the MB removal percentage augmented from 54.21 to 99.45% and the value of q_e also improved from 102.85 to 249.45 mg/g. However, when the activation temperature was further increased from 600°C to 700°C, the MB removal percentage dropped from 99.45 to 70.32% and the value of q_e decreased from 249.45 to 174.34 mg/g (Fig. 2(b)). At higher temperature, the precursor biomass and KOH mixture might have reacted as $6\text{KOH} + 2\text{C} = 2\text{K} + \text{K}_2\text{CO}_3 + 3\text{H}_2$, which might have resulted in the formation and wider pores in the carbon structure. From Fig. 2(c), it is seen that the activation time of 120 min was suitable for activation of precursor and the creation of porous structure. If the residence time was kept more than 120 min, the MB removal percentage and the value of q_e dropped, probably due to extra widening of the mesopore structure.

The yield of activated carbon which was prepared at 600°C with impregnation ratio 2:1 and at 120 min of activation time was 16.78%. The yield of activated carbon was affected by all three process parameters. But the effect of activation temperature on the yield was higher than other two. The yield dropped from 22.56 to

11.42% by increasing temperature from 500°C to 700°C and the yield also dropped from 18.23 to 15.97% by raising impregnation ratio from 1:1 to 3:1. A similar decrease in yield from 17.84 to 16.20% was observed by increasing activation time from 60 min to 150 min.

Characterization of MHAC and millet cob powder biomass

The proximate and ultimate analysis of the porous carbon derived from millet cob powder and raw millet cob biomass are presented in Table 2. The lower value of ash content and the moderate value of fixed carbon of biomass suggests the suitability as a precursor for the production of activated carbon. Ultimate analysis shows that powdered millet cob husk has 44.32% of C, 5.88 % H and 30.40 % O. Not only the experimental conditions affected the properties of derived porous carbon but the composition of precursor was also equally

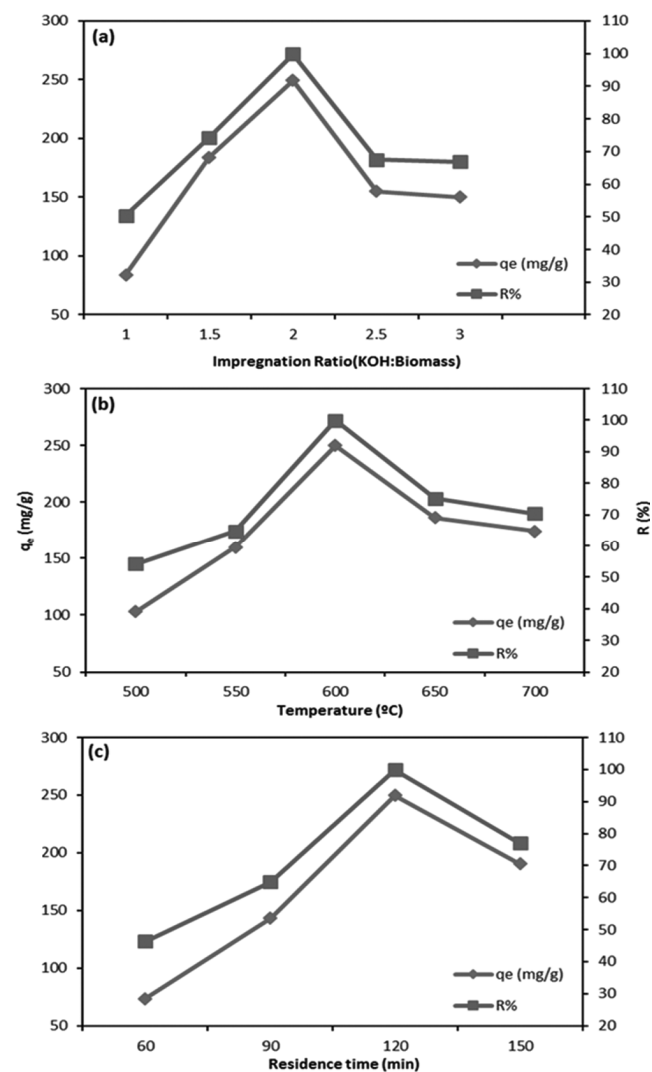


Fig. 2 — Effect of activation conditions on MB adsorption. (a) impregnation ratio, (b) activation temperature and (c) residence time

important for the development of porous structure in the final product. The high carbon content (75.22 %) was a positive attribute of the prepared MHAC.

The FT-IR spectra of millet cob husk (raw biomass), MHAC and CAC were obtained. Both the raw biomass and MHAC displayed bands in the region of 3650-3200 cm^{-1} which represents stretching vibration of hydrogen bonds and water impurities. The higher intensity peak of the millet cob husk at 2926 cm^{-1} indicated the presence of C-H group and band at 1736 cm^{-1} corresponded to the stretching of ketone, aldehyde, and carboxylic acid groups in the raw biomass-present probably as hemicellulose. In addition, a large number of peaks could be detected from 1300 to 1000 cm^{-1} in the raw millet cob husk. These could be attributed to oxygenated compounds of alcohol, ether, ester and phenol category. 1550-1350 cm^{-1} in the raw biomass represented the $-\text{NO}_2$ (stretching) and peaks from 1450-1375 cm^{-1} represented alkanes and C-H (bending). 900-690 cm^{-1} in the raw biomass indicated presence of aromatics too. A noticeable change is observed in the spectra of MHAC compared to spectra of precursor in the bands of two

regions - 1000 to 1750 cm^{-1} and 2800 to 3500 cm^{-1} . In these two regions, the intensities of bands were sharply reduced which suggested that many weak bonds disappeared during activation process. The peaks at 1736 cm^{-1} , 1425 cm^{-1} , 1248 cm^{-1} , 1325 cm^{-1} and 1043 cm^{-1} which represents oxygenated compounds were absent in the spectra of MHAC. The band at 1736 cm^{-1} which probably corresponds to C=O stretch in aldehydes was found only in precursor but not in MHAC. This may be due to thermal sensitivity of ketone and aldehyde groups at high temperature. Similarity in FT-IR spectra was observed in case of CAC, showing that MHAC formed by the present process was at par with commercial grade activated carbon.

Surface morphology of raw biomass and MHAC

Figure 3 shows the SEM images of precursor, MHAC and CAC, respectively. The surface of precursor was comparatively smooth and had very few small pores but noticeable and well-developed structure of pores was observed on the surface of MHAC. As the KOH molecules diffused into the pore, this probably enhanced the carbon-KOH reactions, and hence more pores were created on the surface of MHAC. At high temperature, K_2O was formed by dehydration of KOH and it reacted with CO_2 which was produced by the water-shift reaction and formed K_2CO_3 . Probably metallic potassium intercalation was responsible for the widening of pores and therefore development of large surface area with high pore volume.

As observed in Table 3, the chemical activation of the millet cob husk resulted in activated carbon

Table 2 — Proximate and ultimate analysis of the MHAC and the millet cob powder

	MHAC	Powdered millet cob husk
Proximate analysis (wt %)		
Moisture	5.13	9.90
Volatile matter	24.88	70.43
Fixed carbon	62.49	9.89
Ash	7.50	8.78
Ultimate analysis (wt %)		
Carbon	75.22	44.32
Hydrogen	3.87	5.88
Oxygen	7.76	30.40
Nitrogen	0.52	0.69
Sulfur	0.00	0.03
Ash+Moisture	12.63	18.68

Table 3 — Surface characterization of MHAC obtained from the raw biomass

Type	BET surface area (m^2/g)	Pore volume (cm^3/g)
Millet cob husk powder	0.42	$\ll 0.001$
MHAC	1342	0.99

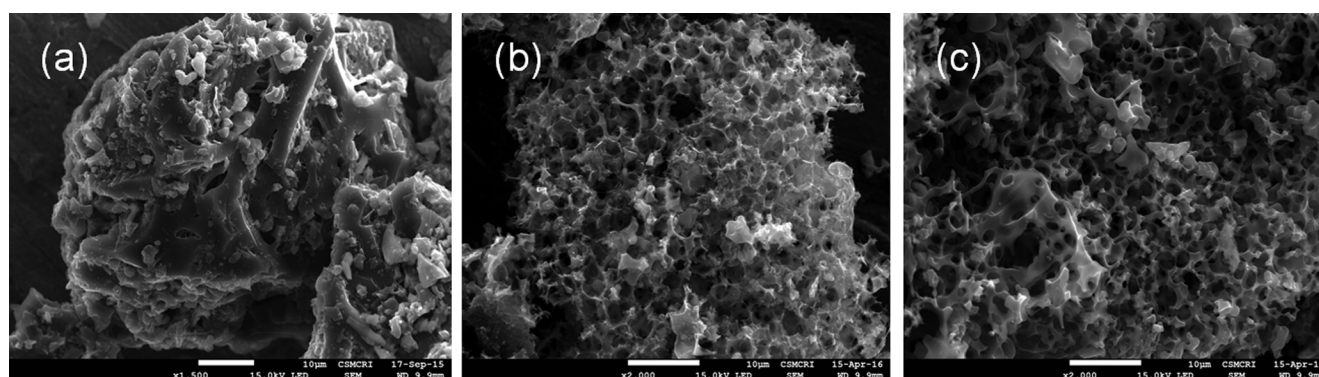


Fig. 3 — SEM images of (a) raw biomass -powdered millet cob husk, (b) CAC and (c) MHAC

having surface area of 1342 m²/g which is almost double the surface area of CAC.

Adsorption of MB by the precursor, MHAC and CAC

Figure 4 shows the adsorption of MB from its solution by millet cob powder, MHAC and CAC with initial concentration of MB was 250 mg/L. The results indicate that the value of adsorption capacity of MHAC was found to be 249.19 mg/g which was higher than the equilibrium adsorption capacity of CAC (238.09 mg/g). This value was also higher than previously reported work²⁶⁻²⁹. The MB removal percentage by MHAC at initial concentration of 250 mg/L was 99.34%. The high surface area of MHAC compared to raw biomass was the cause.

Effects of initial MB concentration on time of adsorption for MHAC

Figure 5 indicates the effect of initial concentration of MB on the adsorption capacity of MHAC. For this study, different initial concentration of MB solution

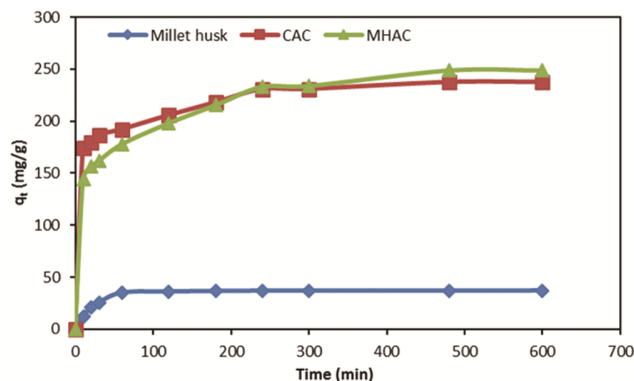


Fig. 4 — Adsorption of MB from solution (250 mgL⁻¹) by millet cob husk, CAC and MHAC

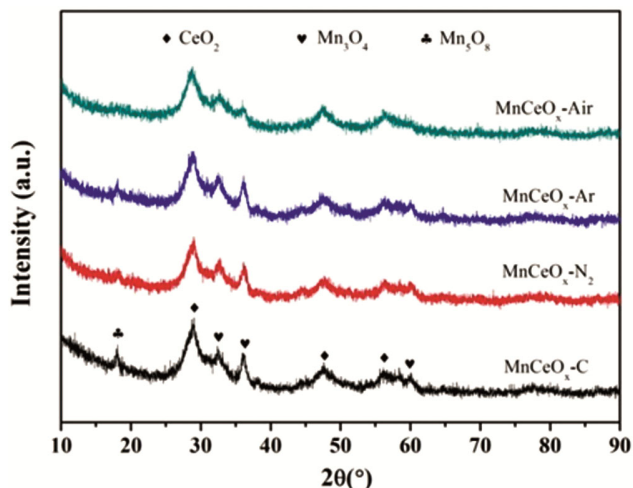


Fig. 5 — Effect of initial concentration on the adsorption of MB from its solution

was taken. It was observed that the adsorption increased quickly in the initial 15-20 min and then it became slower until the equilibrium condition was reached. As the initial concentration was raised from 100 to 500 mg/L, the equilibrium adsorption capacity, q_e increased from 99.72 to 337.21 mg/g. This was because when the concentration of MB in solution increased; the concentration gradient which is the driving force for mass transfer became higher giving higher adsorption of MB. At lower initial concentration, the availability of active vacant sites on the activated carbon was sufficient for the MB molecules adsorption, and also additional vacant sites were probably present.

Effects of solution pH

The adsorption process highly depended on the pH of the solution. For this study, the range of pH selected was 2.0 to 10.0. The MB removal percentage increased with increasing pH from 2.0 to 7.0 and then remained almost unchanged for pH 7.0 to 9. Hence, it is clear that the alkaline or neutral condition of the solution was favourable than acidic condition for the adsorption of MB by MHAC. For this study, 100 mL MB solution (250 mg/L) and 0.1 g MHAC were taken. It is probable that in the lower pH range, lower percentage of MB removal exhibited formation of a weakened charge at the MHAC surface which decreased the electrostatic force for adsorption. But in alkaline medium, the polarity of MHAC changed because of the formation of electric double layer and therefore MB removal percentage increased⁴⁰.

Adsorption Isotherms

Figure 6 shows the linear curves of four different isotherm models for the adsorption of MB by MHAC compared to CAC. The calculated values of each isotherms parameters and value of R^2 are also given in Table 4. The results indicate that the suitability of Langmuir model was moderately higher than Freundlich model. As a result, it may be assumed that the adsorption of MB by MHAC followed a monolayer adsorption on relatively homogeneous surface sites. Also the value of separation factor R_L was <1 which indicates favourable adsorption of MB by the MHAC. Furthermore, the calculated value of heat of sorption obtained in D-R isotherm was 10 kJ/mol, which indicates physical adsorption at the respective sites.

Adsorption Kinetics

The nature of adsorbent and the mass transport between the phases are important parameters to study the adsorption mechanism. Three different kinetic

model linear plots are presented in Fig. 7. The values of different kinetic parameters were computed using intercepts and slopes of various plots are shown in Table 5. The results indicated that the MB adsorption by MHAC was better described by pseudo-second-order kinetic model.

One active site on the surface of adsorbent for single adsorbate molecule is the assumption of the pseudo-first order equation, while two active sites for the adsorption of single adsorbate is the assumption of

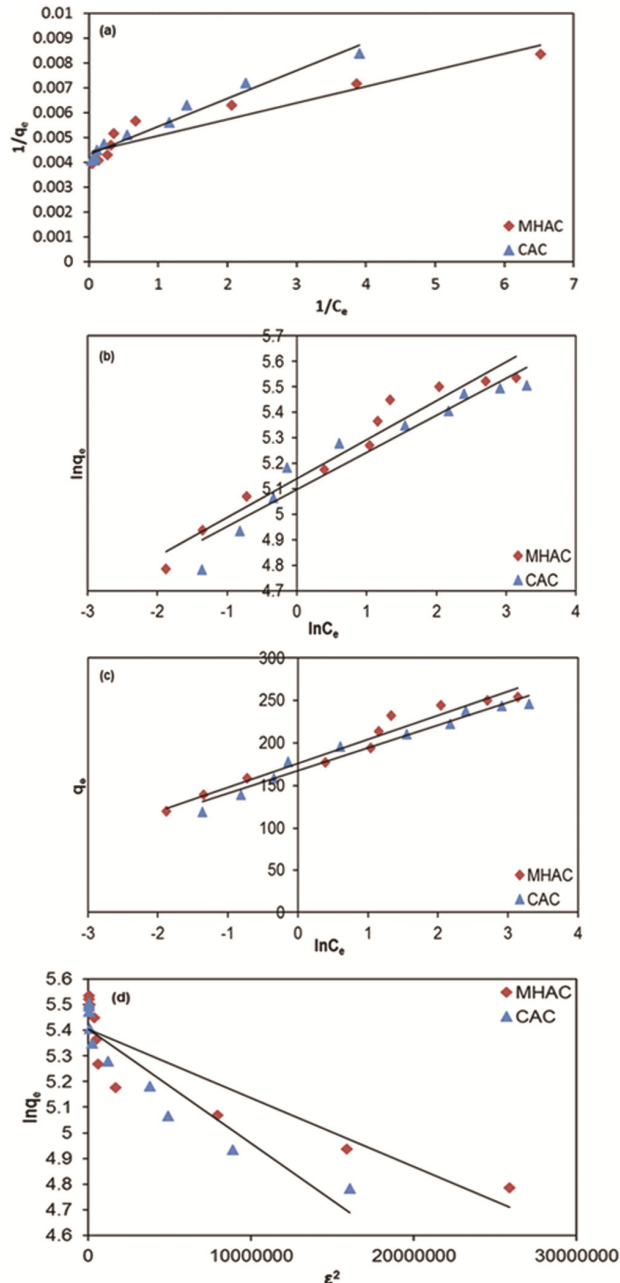


Fig. 6 — Isotherm plots (a) Langmuir (b) Freundlich (c) Temkin and (d) D-R

the pseudo-second order equation. The rate of adsorption of MB by MHAC was fast at initial stage. This may be due to higher concentration gradient. After a while, the rate of adsorption became slower and then it slowly increased till the equilibrium of adsorption was achieved. Initially, the quantity of active sites on the surface of MHAC was more and also the concentration of MB in liquid phase was high, therefore adsorption was fast. According to the results, the adsorption process might be physisorption as well as chemisorption.

There is a straight relationship between the adsorbed dye quantity and the square root of time which is the assumption of the intraparticle diffusion kinetic model. From the Fig. 7(c), the lines did not

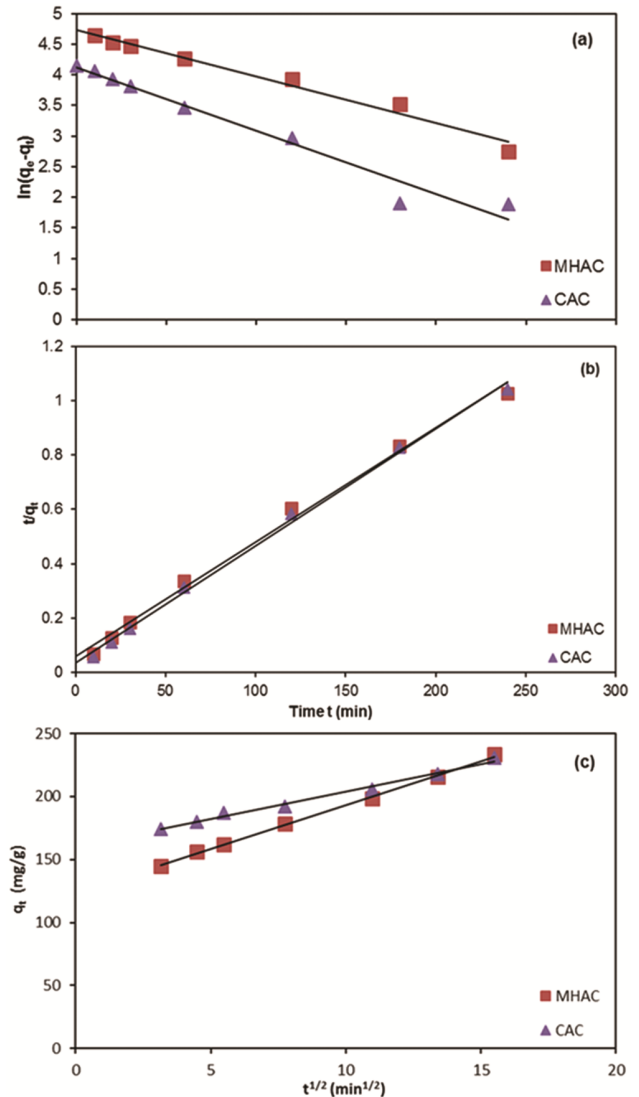


Fig. 7 — Linear regression curves of (a) pseudo first order, (b) pseudo second order and (c) intraparticle diffusion for adsorption removal of MB

meet at the origin which signifies the fact that the intraparticle diffusion was not only the rate limiting step for the adsorption process.

Thermodynamic Modeling

The concept of thermodynamics assumes that the change in entropy is the driving force in an isolated system. The behaviour of adsorption process could be determined by the change in thermodynamic properties like standard enthalpy (ΔH^0), standard entropy (ΔS^0) and standard Gibbs free energy (ΔG^0).

The value of ΔH^0 and ΔS^0 could be computed using the following equation,

$$\ln K_c = \frac{\Delta S^0}{R} - \frac{\Delta H^0}{RT} \quad \dots (13)$$

where, T (K) is the temperature of solution, R is the gas constant (8.314 J/mol.K) and $K_c = C_i/C_e$ is the equilibrium constant.

The values of ΔH^0 and ΔS^0 were computed from the Van't Hoff plot between $\ln K_c$ vs. $1/T$ as shown in Fig. 8. ΔG^0 could then be calculated using the relation below,

$$\Delta G^0 = -RT \ln K_c \quad \dots (14)$$

The negative value of ΔG^0 and ΔH^0 indicates that the adsorption of MB by MHAC was a spontaneous and an exothermic process. The negative value of ΔS^0 shows that the process of adsorption was completed with minor disorder in the system (Table 6).

Regeneration studies of the used MHAC

In this study, 250 mg/L of MB solution (1L) was initially treated with 1g of MHAC which is denoted as Stage 1. The exhausted MHAC was treated with varying concentrations of NaOH (0.1N to 0.5N) to find out the optimum condition for regeneration. It was found that the 0.2N NaOH solution was the optimum concentration. The resultant solution was filtered, neutralized and dried. The regenerated MHAC was then used for next stage adsorption. Five cycles were repeated using the same process. Loss of adsorption ability of MHAC during regeneration was very less and in the final stage 85.34 % of MB was absorbed by the spent activated carbon, which was again regenerated successfully for further application.

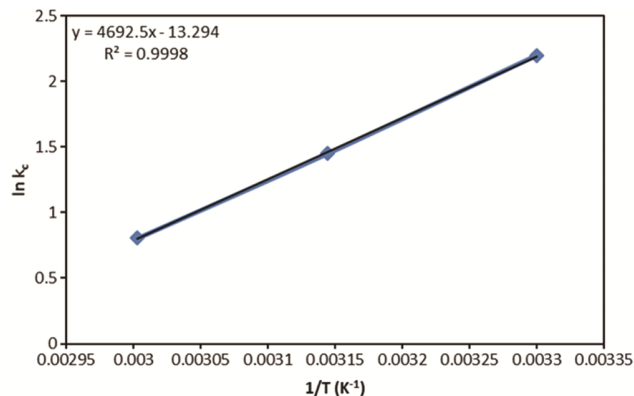


Fig. 8 — Van't Hoff plot for adsorption of MB by MHAC

Table 4 — Isothermal parameters for adsorption of MB by MHAC and CAC

Isotherms	Adsorbent	Constants			R^2
		Q_0 (mg/g)	R_L	K_L (L/mg)	
Langmuir isotherm $\frac{1}{q_e} = \frac{1}{Q_0} + \frac{1}{Q_0 K_L C_e}$	MHAC	250	0.001664	4.00	0.972
	CAC	250	0.001664	4.00	0.965
Freundlich isotherm $\ln q_e = \ln K_f + \frac{1}{n} \ln C_e$		K_f	$1/n$	N	
	MHAC	170.88	6.579	0.1519	0.949
	CAC	163.69	6.8966	0.1449	0.923
Temkin isotherm $q_e = \frac{RT}{b_T} \ln A_T + \frac{RT}{b_T} \ln C_e$		A_T (L/mg)	b_T	B (J/mol)	
	MHAC	530.6	89.649	28.10	0.958
	CAC	545.21	94.6	26.63	0.961
Dubinin–Radushkevich isotherm $\ln q_e = \ln q_s - K_{DR} \varepsilon^2$		q_s (mg/g)	E (J/mol)	K_{DR} (mol ² /J ²)	
	MHAC	221.85	4082.48	3×10^{-8}	0.816
	CAC	222.29	3535.53	4×10^{-8}	0.89

Table 5 — Estimated kinetic constants for adsorption of MB by MHAC

$q_{e,exp}$ (mg/g)	Pseudo-first-order			Pseudo-second-order			Intraparticle diffusion			
	K_1 (h ⁻¹)	$q_{e,cal}$ (mg/g)	R^2	K_2 (g/mg.h)	$q_{e,cal}$ (mg/g)	R^2	k_{int} (mg/gh ^{1/2})	C_i	R^2	
MHAC	248.35	0.42	109.84	0.97	0.015	250	0.99	0.85	126	0.99
CAC	245.86	0.48	71.09	0.95	0.025	250	0.99	0.54	161.4	0.98

Table 6 — Thermodynamic parameters for adsorption of MB by MHAC

T(K)	ΔG^0 (kJ/mol)	ΔH^0 (kJ/mol)	ΔS^0 (J/mol.K)
303	-5539.06		
318	-3834.6	-39.009	-110.493
333	-2226.37		

Table 7 — Adsorption and desorption cycles of MB by MHAC

Sample Stage	MB adsorption (%)	MB (%) recovered
1	99.13	96.25
2	95.43	92.82
3	90.86	88.21
4	87.09	84.35
5	85.34	81.76

Table 7 gives the adsorption and recovered % of MB by MHAC.

Conclusion

This study affirms that the prepared MHAC from locally, freely and amply available agricultural waste of millet cob husk biomass can be an appropriate option of non-renewable source based activated carbon for the adsorption of MB dye from its aqueous solutions. The MHAC was prepared in a single step from the biomass at a temperature of 600°C, impregnation ratio of 2:1 and consolidated time of 120 min. The BET surface area of MHAC was 1342 m²/g and the FT-IR spectra and SEM images were similar to CAC. Neutral or alkaline pH was favourable for adsorption of MB onto MHAC. Langmuir and Temkin models fitted better with the equilibrium data and the adsorption kinetics data was well described by the pseudo-second-order kinetic model. Thermodynamic properties suggested that the adsorption phenomenon was spontaneous, exothermic and decreased the disorder degree of the process. Regeneration of the carbon was carried out for five cycles. 85.34 % MB could be absorbed by the spent carbon, after fifth cycle.

References

- Easton J R, Waters B D, Churchley J H & Harrison J, *Colour in Dyehouse Effluent, Society of Dyers and Colorists* (The Alden Press, Oxford), 1995, 9.
- Correia V M, Stephenson T & Judd S J, *Environ Technol*, 15 (1994) 917.
- Liang C Z, Sun S P, Li F Y, Ong Y K & Chung T S, *J Membr Sci*, 469 (2014) 306.
- Bakheet B, Yuan S, Li Z, Wang H, Zuo, J, Komarneni S & Wang Y, *Water Res*, 47 (2013) 6234.
- Del Rio A I, Fernandez J, Molina J, Bonastre J & Cases F, *Desalination*, 273 (2011) 428.
- Kumar P, Agnihotri R & Mondal M K, *J Environ Chem Eng*, 1 (2013) 440.
- Liu C, Hsieh Y, Lai P, Li C & Kao C, *Dyes Pigm*, 68 (2006) 191.
- Tichonovas M, Krugly E, Racys V, Hippler R, Kauneliene V, Stasiulaitiene I & Martuzevicius D, *Chem Eng J*, 229 (2013) 9.
- Turgay O, Ersoz G, Atalay S, Forss J & Welander U, *Sep Purif Technol*, 79 (2011) 26.
- Kaouah F, Boumaza T, Trari M & Bendjama Z, *J Clean Prod*, 54 (2013) 296.
- Emami Z & Azizian S, *J Anal Appl Pyrolysis*, 108 (2014) 176.
- Omri A, Benzina M & Ammar N, *J Ind Eng Chem*, 19 (2013) 2092.
- Gonzalez P G, Hernandez-Quiroz T & Garcia-Gonzalez L, *Fuel Process Technol*, 127 (2014) 133.
- Liu Q Y, Ai H, Meng M W, Wei Y L, Liu M D & Deng X M, *Environ Protec Chem Ind*, 32 (2012) 561.
- Tongpoothorn W, Sriuttha M, Homchan P, Chanthai S & Ruangviriyachai C, *Chem Eng Res Des*, 89 (2011) 335.
- Zhong Z Y, Yang Q, Li X M, Luo K, Liu Y & Zeng G M, *Ind Crops Prod*, 37 (2012) 178.
- Foo K, Y & Hameed B H, *Bioresour Technol*, 116 (2012) 522.
- Gao Q, Liu H, Cheng C, Li K, Zhang J, Zhang C & Li Y, *Powder Technol*, 249 (2013) 234.
- Karagoz S, Tay T, Ucar S & Erdem M, *Bioresour Technol*, 99 (2008) 6214.
- Ouid-Idriss A, Stitou A, Cuerda-correa A & Macias-Garda A, *Fuel Process Technol*, 92 (2011) 261.
- Singh K & Chandra B, *Indian J Chem Technol*, 22 (2015) 11.
- El-Shafey E I, Syeda N F A, Saleh A & Haider A J A, *J Environ Chem Eng*, 4 (2016) 2713.
- Shukla A, Lalit A, Sharma V, Vats S & Alam A, *J App Research*, 2015, 1 (2015) 59.
- Hiloidhari M, Das D & Baruah D C, *Renew Sust Energ Rev*, 32 (2014) 504.
- Tamilselvi S, Asaithambi M & Sivakumar V, *Indian J Chem Technol*, 23 (2016) 497.
- Jansi Rani M, Murugan M, Subramanian P & Subramanian E, *Indian J Chem Technol*, 23 (2016) 22.
- Cigdem S O, *Physicochem Probl Mi Process*, 48 (2012) 441.
- Gao J J, Qin Y B, Zhou T, Cao D D, Xin P, Hochsetter D & Wang Y F, *J Zhejiang Univ Sci B*, 14 (2013) 650.
- Ismail M N, Aziz H A, Ahmad M A & Kamaruddin M A, *Inter J Sci Res Knowled*, 1 (2013) 388.
- Thitame P V & Shukla S R, *Chem Eng Commun*, 203 (2016) 791.
- Amin N K, *Desalination*, 223 (2008) 152.
- Namasivayam C & Kavitha D, *Dyes pigm*, 54 (2002) 47.
- Langmuir I, *J Am Chem Soc*, 40 (1918) 1361.
- Freundlich H, *J Phys Chem*, 57 (1906) 387.
- Temkin M J & Pyzhev V, *Acta Physiochim*, USSR 12 (1940) 217.
- Dubinini M M, *Zhurnal Fizicheskoi Khimii*, 39 (1965) 1305.
- Langergren S & Svenska B K, *VeternskapsakadHandl*, 24 (1898) 1.
- Ho Y S & McKay G, *Can J Chem Eng*, 76 (1998) 822.
- Jr. Weber W J & Morris J C, *J Sanit Eng Div*, ASCE 18 (1963) 31.
- Hameed B H & El-khaiary M L, *J Hazard Mater*, 157 (2008) 344.